



HAL
open science

Cytotoxic and genotoxic effects of epoxiconazole on F98 glioma cells

Hiba Hamdi, Salwa Abid-Essefi, Joël Eyer

► **To cite this version:**

Hiba Hamdi, Salwa Abid-Essefi, Joël Eyer. Cytotoxic and genotoxic effects of epoxiconazole on F98 glioma cells. *Chemosphere*, 2019, 229, pp.314-323. 10.1016/j.chemosphere.2019.05.018. hal-02616076

HAL Id: hal-02616076

<https://univ-angers.hal.science/hal-02616076>

Submitted on 22 Oct 2021

HAL is a multi-disciplinary open access archive for the deposit and dissemination of scientific research documents, whether they are published or not. The documents may come from teaching and research institutions in France or abroad, or from public or private research centers.

L'archive ouverte pluridisciplinaire **HAL**, est destinée au dépôt et à la diffusion de documents scientifiques de niveau recherche, publiés ou non, émanant des établissements d'enseignement et de recherche français ou étrangers, des laboratoires publics ou privés.



Distributed under a Creative Commons Attribution - NonCommercial 4.0 International License

1 **Cytotoxic and genotoxic effects of Epoxiconazole on F98 glioma cells**

2

3 Hiba Hamdi ^{a, b}, Salwa Abid-Essefi ^a, Joel Eyer ^{c *}

4

5

6 ^a Laboratory for Research on Biologically Compatible Compounds, Faculty of Dental Medicine,
7 University of Monastir, Avicenne Street, 5019 Monastir, Tunisia.

8 ^b Higher Institute of Biotechnology, University of Monastir, Tunisia.

9 ^c Laboratoire Micro et Nanomédecines Translationnelles (MINT), Inserm 1066, CNRS 6021, Institut
10 de Biologie de la Santé, Centre Hospitalier Universitaire, 49033 Angers, France.

11

12

13 ***Corresponding author: Joel Eyer**

14 E-mail: joel.eyer@univ-angers.fr

15 Tel: 33.(0)2.44.68.84.88

16 Fax: 33.(0)2.44.68.84.89

17

18 **Abbreviations:** EPX: Epoxiconazole; ROS: Reactive oxygen species; $\Delta\Psi_m$: mitochondrial
19 transmembrane potential; IC50: Inhibitory concentration of 50% of the population; PBS: Phosphate
20 buffer saline; DCFH-DA: 2, 7-Dichlorofluoresce diacetate; FCS: Fetal calf serum; MTT: 3-4, 5-
21 Dimethylthiazol-2-yl, 2, 5-diphenyltetrazolium bromide; NAC: N-acetylcysteine; LMA: Low melting
22 point agarose; NMA: Normal melting point agarose; DMSO: Dimethylsulfoxide; PI: Propidium
23 iodide; BSA: Bovine serum albumin; DAPI: 496-Diaminido-2-phenylindole; Rh-123: Rhodamine 123;
24 AO: Acridine orange; EB: Ethidium bromide; H₂O₂: Hydrogen peroxide; MDA: Malondialdehyde;
25 SDS: Sodium dodecyl sulfate; KCL: Potassium chloride; DO: Optical density; GSH: Glutathione.

26

27

28

29

30 **Highlights:**

- 31 • EPX induces cytotoxic effects in F98 glioma cells
- 32 • EPX produces cell cycle arrest, cytoskeleton disruption, DNA damage
- 33 • EPX affects mitochondrial function and induces apoptosis via caspases dependent
- 34 signaling pathway in F98 cells
- 35 • EPX provokes ROS generation and lipid peroxidation

36

37 **Abstract**

38 Epoxiconazole (EPX) is a very effective fungicide of the triazole family. Given its wide
39 spectrum of use, the increased application of this pesticide may represent a serious risk on
40 human health. Previous studies have found that EPX is cytotoxic to cells, although the exact
41 mechanism remains elusive. In particular, the effect on the nervous system is poorly
42 elucidated. Here we evaluated the implication of oxidative stress in the neurotoxicity and
43 studied its apoptotic mechanism of action. We demonstrated that the treatment by EPX
44 reduces the viability of cells in a dose dependent manner with an IC₅₀ of 50 μM. It also
45 provokes the reduction of cell proliferation. EPX could trigger arrest in G1/S phase of cell
46 cycle with low doses, however with IC₅₀, it induced an accumulation of F98 cells in G2/M
47 phase. Moreover, EPX induced cytoskeleton disruption as evidenced by immunocytochemical
48 analysis. It provoked also DNA fragmentation in a concentration dependent manner. The EPX
49 induced apoptosis, which was observed by morphological changes and by positive Annexin V
50 FITC-PI staining concurrent with a depolarization of mitochondria. Furthermore, the cell
51 mortality provoked by EPX was significantly reduced by pretreatment with Z-VAD-FMK, a
52 caspase inhibitor. Moreover, N-acetylcysteine (NAC) strongly restores cell viability that has
53 been inhibited by EPX. The results of these findings highlight the implication of ROS
54 generation in the neurotoxicity induced by EPX, indicating that the production of ROS is the
55 main cause of the induction of apoptosis probably via the mitochondrial pathway.

56 **Keywords**

57 Epoxiconazole; F98 cells; Cell cycle arrest; Cytoskeleton; ROS; Mitochondria; Apoptosis.

58

59 1. Introduction

60 The emergence of crop pests has significantly increased the application of pesticides as a
61 solution and effective method of control. Despite their effectiveness, these products pose a
62 real risk of contamination for non-target organisms and constitute a great threat to
63 ecosystems. Exposure to these pollutants can be done in two ways, either by draining the
64 contaminant or by handling incorrectly the material of application (De Wilde et al., 2007;
65 Karanasios et al., 2012). Human exposure to pesticides can occur through three routes,
66 namely, dermal absorption, inhalation, and ingestion (Toni et al., 2011; El-Amrani et al.,
67 2012). Due to the increased agricultural use of these chemicals, their residues are dispersed in
68 water and in food supply. Amongst these products, triazole fungicides represent some of the
69 most important group of fungicides (Verweij et al., 2013). Triazoles are widely applied in
70 agriculture for cereals' treatment, vegetables, fruits and flowers and also as medical products
71 (Hester et al., 2012). The mechanism of action of this group of fungicides is based on the
72 inhibition of lanosterol 14 α -demethylase (CYP51), an enzyme essential in maintaining the
73 integrity of the fungal membrane (Ghannoum and Rice, 1999; Tully et al., 2006). In addition,
74 EPA (2006) has demonstrated that triazoles can cause serious harm to human and animal
75 health, particularly the nervous system, including neuronal degeneration and prenatal stress
76 (PNS) (EPA, 2006). However, the exact pathways involved in the neurotoxicity induced by
77 triazole fungicides are not well characterized.

78 Epoxiconazole (EPX) is a triazole fungicide commonly applied in the control of fungal
79 diseases in agriculture, but its mechanism of action is not based solely on the inhibition of
80 fungal enzyme but may also inhibit other cytochromes (CYP), including cytochrome P450
81 and this can cause various health problems for non-target organisms (Wuttke et al., 2001;
82 Trosken et al., 2004). Oxidative stress is the imbalance between pro-oxidant and anti-oxidant
83 ratio. Its production causes harm to biological macromolecules such as lipids, proteins and
84 DNA. In particular, the excessive production of ROS can cause serious disorganization in the
85 cellular structure (Barzilai and Yamamoto, 2004). Oxidative stress is crucial for the induction
86 of apoptosis (Livingstone, 2001). It has been shown that the toxicity of triazole fungicides
87 passes through oxidative stress, causing DNA damage or apoptosis (Ross et al., 2009, 2012;
88 Hester et al., 2006, 2012). Other pathways are involved in the inhibitory effect of triazole
89 fungicides, such as cell cycle dysregulation (Schwarzbacherová et al., 2017; Šiviková et al.,
90 2018).

91 Finally, many studies have shown the primordial role of the cytoskeleton and its organization
92 in controlling programmed cell death (Gourlay and Ayscough, 2005, Ndozangue-Touriguine
93 et al., 2008). The cytoskeleton is formed by three type of filament: microfilaments (MF),
94 microtubules (MT) and intermediate filaments (IF). These filaments play key roles in the
95 conservation of cell architecture, its internal organization, the cellular form, the motility and
96 many other interactions (Hooser et al., 1991, Ding et al., 2000b). Disruption of the
97 cytoskeletal network could provoke the loss of balance and integrity of the cell membrane (Li
98 et al., 2001; Alverca et al., 2009).

99

100 Despite the massive use of EPX in agriculture and the high risk of exposure of the human and
101 animal population to this fungicide, there is a lack of data on its impact on the body and
102 especially on the brain. For this reason, our study aims to better elucidate the mechanism of
103 action of EPX on F98 glioma cells with a special reference to the implication of oxidative
104 stress in the neurotoxicity produced by this product. We have chosen F98 cells because this
105 model of cells exhibits features of the human glioblastoma in its aggressiveness, histological
106 appearance and lack of immunogenicity, and through genetic transfection and
107 bioluminescence imaging, we are able to follow day-to-day in vivo progress of the tumour
108 without limitation. We have also used these cells mainly because of their large size necessary
109 to determine the effects of EPX on organelles, in particular the cytoskeleton and
110 mitochondria.

111

112

113

114

115 **2. Materials and methods**

116

117 **2.1. Chemicals**

118

119 Epoxiconazole, ZVAD-fmk, N-acetylcysteine (NAC), Low melting point agarose (LMA),
120 Normal melting point agarose (NMA), Sodium dodecyl sulfate (SDS), Potassium chloride
121 (KCl) and Bovine serum albumin (BSA), were purchased from Sigma–Aldrich (St. Louis,
122 MO, USA). 3-(4, 5-Dimethylthiazol-2-yl), 2, 5-diphenyltetrazolium bromide (MTT), Cell
123 culture medium (DMEM), Fetal calf serum (FCS), Phosphate buffer saline (PBS), Trypsin
124 EDTA, Penicillin and streptomycin mixture and NEAA (200 mM) were from GIBCO-BCL
125 (UK). 2, 7-Dichlorofluoresce diacetate (DCFH-DA) was supplied by Molecular Probes
126 (Cergy Pontoise, France).

127

128 **2.2. Cell culture**

129

130 Rat glioma cells (F98) were cultured in DMEM, supplemented with 10% FCS, 1% NEAA,
131 1% of mixture penicillin and streptomycin at 37 °C with 5% CO₂.

132

133 **2.3. Cell viability analysis by MTT test**

134

135 F98 cells were seeded (2 × 10⁴ cells/well in 96-well plates) in complete DMEM medium. After
136 incubation for 24 hours at 37 °C with 5% CO₂, the medium was renewed and the cells in the
137 exponential phase of growth were treated with EPX at the desired concentrations (5-150 μM),
138 then, incubated for 24 hours at 37 °C. At the end of this incubation, the medium containing
139 the pesticide was removed and the cell layer was rinsed 3 times with PBS. A solution of MTT
140 (0.5 mg ml⁻¹) in complete DMEM medium was added to cells for 3 h. Then, the MTT solution
141 was removed and the insoluble formazan crystals formed were dissolved in a lysis solution
142 containing dimethylsulfoxide (DMSO). Finally, absorbance was measured at 540 nm, and the
143 percentage of viability at each EPX concentration was determined relative to the control cells.
144 The EPX concentrations were chosen according to the IC₅₀ (Inhibitory Concentration of 50%
145 of the population).

146

147 **2.4. Study of cell proliferation by cell cycle analysis**

148

149 The F98 cells were seeded at 5×10^5 cells/well and cultured for 24 hours. Afterwards, the cells
150 were treated with EPX at the indicated doses ($12 \mu\text{M}$ ($1/4$ IC₅₀), $25 \mu\text{M}$ ($1/2$ IC₅₀ and $50 \mu\text{M}$
151 (IC₅₀)) for 24 hours. Then, the cells were detached by trypsin, centrifuged for 2 min at 2500
152 rpm and washed with PBS 0.1% tween. After fixation with Ethanol 70%, the samples were
153 centrifuged and washed with PBS. After the addition of RNase (1 mg ml^{-1}), the cells were
154 incubated at 37°C for 30 min in dark. Finally, $400 \mu\text{l}$ propidium iodide (PI, $10 \mu\text{g ml}^{-1}$) was
155 added. The cell cycle arrest was analyzed by flow cytometer. The percentages of cell
156 Distribution in G₁, S and G₂/M phases were evaluated by using WinMDI 2.9 (Mirzaa et al.,
157 2018).

158

159 **2.5. Immunocytochemistry**

160

161 After seeding of F98 cells into 24-well plates (3×10^4 cells / well) containing coverslips, the
162 cells were treated with increased concentrations of EPX and incubated during 6 hours at
163 37°C . Then, the cells were washed with PBS, fixed in 4% paraformaldehyde and washed 3
164 times in PBS. Afterwards, the cells were incubated in a 30% triton X-100 permeabilization
165 solution and washed 3 times in PBS. After staining with a $50 \mu\text{g ml}^{-1}$ fluorescent phalloidin
166 conjugate solution in PBS, the F98 cells were incubated in a blocking solution (5% BSA), and
167 then incubated overnight with mouse anti-alpha-tubulin antibody or anti-mouse vimentin
168 antibody. The localization of tubulin or vimentin was done by the use of an anti-mouse Alexa
169 antibody of 568 nm for 1 hour, followed by washing in PBS. In order to visualize the nucleus,
170 the samples were counterstained with $3 \mu\text{M}$ 496-diaminido-2-phenylindole (DAPI) and
171 washed twice in PBS. Finally, the coverslips were mounted with an anti-fading solution and
172 images were taken with an Olympus confocal microscope (BX50) using Fluoview.3.1.
173 program, or an inverted microscope Leica DMI 6000 and analyzed with Metamorph 7.1.7.0.
174 (Balzeau et al., 2012).

175

176 **2.6. DNA fragmentation assessed by the comet assay**

177

178 After treatment of the cells with increasing concentrations of EPX, the cell suspensions
179 containing 2×10^4 cells were mixed with 0.06 ml of low melting point agarose at 1% in PBS.
180 Then, 0.110 ml of the solution obtained were deposited in thin layers on slides, previously
181 covered with a 1% agarose underlayer and allowed to dry during 10 min. The slides were then

182 soaked in a freshly prepared lysis buffer. After one hour of incubation at 4 °C, the slides were
183 immersed in the electrophoresis buffer for 20 min, followed by 15 min of migration under a
184 voltage of 25 V (300 mA). After electrophoresis, the slides were rinsed with the neutralization
185 buffer 3 times for 5 min, and drained gently. 0.050 ml of ethidium bromide (20 µg ml⁻¹) were
186 then deposited on each slide and then covered with a coverslip in order to observe them under
187 a fluorescence microscope. A visual count was made on 150 comets per blade according to
188 the intensity of the fluorescence of the tail obtained following the fragmentation of the DNA
189 and then classified into 5 classes; from class 0 (intact nucleoli) to class 4 (totally damaged
190 nucleoli).

191

192

193 **2.7. Mitochondrial membrane potential (MMP) assessment**

194

195 First of all, the cells were seeded in 96-well culture plates. After that, they were under
196 treatment and incubation for 24 hours with different concentrations of EPX. Then, the
197 medium was removed and the cells were incubated with 5 µM of rhodamine 123, and then,
198 the cells were rinsed and re-incubated with PBS. The fluorescence was finally measured using
199 a fluorimeter (Biotek FLx800). The decrease in the intensity of the fluorescence reflects the
200 decrease in the retention of Rh-123 and thus the fall of the mitochondrial potential.

201

202 **2.8. Apoptosis analysis**

203

204 The combination of the two dyes acridine orange (AO) and ethidium bromide (EB) allows the
205 separation between the living cells and the dead ones either by apoptosis or by necrosis (Li et
206 al., 2013). F98 cells were seeded at 10⁶ cells/well of complete medium into 6-well plates and
207 incubated for 24 hours. Later on, the cells were treated with EPX for 24 hours with (5% CO₂
208 – 95% air). After washing them with PBS, they were incubated in a dark environment with
209 the mixture of AO/EB for 15 minutes. Then, they were washed three times with PBS. Finally,
210 they were observed under a fluorescence microscope for taking pictures and counting (200
211 stained cells from each treatment group).

212

213

214

215

216 **2.9. Annexin V-FITC/PI double staining assay**

217

218 After seeding, treatment and incubation, the F98 cells were washed by 1× binding buffer and
219 centrifuged. Then, they were incubated with Annexin V-FITC/PI in the dark. Finally, 5 µl of
220 propidium iodide was added to each sample in order to separate the dead cells by necrosis.
221 The samples were analyzed by flow cytometry (Hu et al., 2015).

222

223 **2.10. Oxidative stress generation**

224

225 Fluorometric analysis using 2, 7-dichlorofluorescein diacetate (DCFH-DA) allows to control
226 oxidation in biological systems and to quantify intracellular ROS (Cathcart et al., 1983;
227 Debbasch et al., 2001 and Gomes et al., 2005). The cells were seeded in multi-well plates (96
228 wells) at the rate of 2×10^4 cells / well. After 24 hours, they were incubated for 30 min with 20
229 µM DCFH-DA and then treated with EPX at increasing concentrations, and incubated for 24
230 hours. H₂O₂ (20 µM) was used as a positive control. The fluorescence was measured using a
231 fluorometer (Biotek FLx800).

232

233 **2.11. Malondialdehyde level measurement**

234

235 Cells were seeded at 10^6 cells / well of complete medium into 6-well plates and incubated for
236 24 hours. Then, they were treated with EPX for 24 hours with (5% CO₂ – 95% air). After the
237 incubation process, the medium was removed, the cell layer was rinsed twice with 0.5 ml of
238 PBS, and the cells became detached from their support by trypsination in which they were
239 recovered and centrifuged (1800 rpm for 10 min). The spectrophotometric assay of MDA was
240 carried out according to the method described by Ohkawa et al (1979). Thus, the pellet was
241 taken up in 0.2 ml KCl 1.15% to which were added 0.2 ml of SDS 8.1%, 1.5 ml of 20% acetic
242 acid adjusted to pH 3.5, 1.5 ml of thiobarbituric acid 0.8%, supplemented with H₂O qsp 4 ml.
243 The samples were heated at 95 °C for 120 min and then cooled to room temperature. 5 ml of a
244 mixture of n-butanol + pyridine (15: 1 v/v) were added to each sample. After vigorous stirring
245 and centrifugation at 1800 rpm for 10 min, the supernatant was isolated and the DO reading
246 was performed at 546 nm.

247

248 **2.12. Statistical analysis**

249

250 Each experiment was repeated at least 3 times under different treatment conditions and data
251 were expressed as the mean \pm SD. Statistical differences between control and EPX-treated
252 groups were evaluated by Student's test. Differences were considered significant at $p < 0.05$.
253

254 **3. Results**

255

256 **3.1. EPX affects the viability of F98 and induces the arrest of their cell cycle followed by** 257 **the activation of apoptosis**

258

259 The viability of F98 cells after 24 hours of treatment by different concentrations of EPX (5-
260 150 μM) was studied by the MTT test and the results of the present study demonstrated that
261 EPX induces a reduction in cell viability in a dose-dependent manner, with an IC_{50} equal to
262 50 μM (Fig. 1.1.A, B). Positive control treated with Colchicine (5 $\mu\text{g}/\text{ml}$) also induces greatly
263 a reduction in cell viability compared to untreated cells (70% of cell death).

264

265 In order to examine the anti-proliferative effect of EPX, the cell cycle of F98 cells has been
266 evaluated. The results showed that the rate of G0/G1 increased with low doses of EPX ($\frac{1}{4}$
267 IC_{50} and $\frac{1}{2}$ IC_{50}), however the rate of G2/M increased with IC_{50} (Fig. 1.2.A and 1.2.B).

268

269 The possible effect of EPX on apoptosis of the F98 cells was evaluated after 24 hours of
270 treatment, and using the AO/EB fluorescent DNA binding dyes (Fig. 1.3.A). The nucleus of
271 the untreated cells was round and unaffected, and the cells were stained green. As EPX doses
272 increased, cells were stained light green with a crescent shape inside the nucleus, indicating
273 that most cells were in the process of apoptotic death. The results indicate that the percentage
274 of apoptosis increased significantly after EPX treatment for 24h in a concentration-dependent
275 manner (Fig. 1.3.B). In addition, we evaluated the externalization of phosphatidyl serine (PS)
276 in F98 cells. The EPX-provoked programmed cell death in F98 cells was further tested by the
277 combination of Annexin-V-FITC and PI. Cells that are in early apoptosis are PI negative and
278 annexin V-FITC positive, whereas cells that are in late apoptosis are positive for both (Fig.
279 1.4.A). The percentage of programmed cell death was analyzed as the sum of early and late
280 apoptosis. As presented in Fig. 1.4.B, an important rate of cells was undergoing apoptosis
281 after treatment by EPX concentrations comparing with control cells. The level of apoptosis in
282 the untreated F98 cells was $5.83 \pm 1.1\%$ and in EPX treated F98 cells was 17.26 ± 1.2 , 30.11
283 ± 0.9 and $41.33 \pm 1.4\%$ at respectively 12, 25 and 50 μM .

284

285 **3.2. EPX destroys the organization of the cytoskeleton**

286

287 The treatment of F98 cells by EPX brought about a profound disruption of cytoskeleton
288 structures and the results are displayed in Fig. 2. In untreated cells, a clear and normal
289 organization of microtubules (Fig. 2.A), intermediate filaments (Fig. 2.B) and actin
290 microfilaments (Fig. 2.C) is observed. After 6 h of treatment by EPX, a remarkable
291 disorganization of MTs, MFs and IFs was observed at $\frac{1}{4}$ IC50 dose. At higher concentration
292 (the $\frac{1}{2}$ IC50 group), most of the MFs and IFs are degraded with formation of aggregates.
293 Finally, the cytoskeleton completely disappeared in the IC50 group.

294

295 **3.3. EPX induces the mitochondrial-mediated apoptotic pathway through the loss of** 296 **MMP ($\Delta\Psi_m$) and caspase activation**

297

298 The mitochondrial membrane potential is proportional to the retention of rhodamine-123
299 within the mitochondria (Cao et al., 2007) and in most of the cases its depolarization is
300 associated with cell death by apoptosis (Wang et al., 2009). The treatment by EPX at the
301 indicated concentrations (12 μ M, 25 μ M and 50 μ M) provoked a reduction in $\Delta\Psi_m$ ($p < 0.05$)
302 (Fig. 3.1).

303

304 In order to determine the possible implication of caspases in the process of apoptotic death,
305 we added the caspase inhibitor ZVAD (50 μ M) during 2 h before treating F98 cells by EPX.
306 Such a pre-treatment with ZVAD-fmk induced a significant inhibition of cell mortality
307 ($P < 0.05$) (Fig. 3.2).

308

309 **3.4. EPX causes oxidative damage through the production of reactive oxygen species** 310 **(ROS) and induces lipid oxidation and DNA fragmentation**

311

312 To evaluate the effect of EPX on the redox status of the cell, the generation of ROS was
313 measured by the DCFH-DA test. As presented in Fig. 4.1, EPX treated cells at these
314 concentrations (12, 25 and 50 μ M) provoked an elevation of ROS production in a
315 concentration-dependent manner ($p < 0.05$). Indeed, we used H_2O_2 (20 μ M) as positive control
316 (20 μ M) and our results showed a significant increase in the ROS rate ($p < 0.001$).

317

318 Lipid oxidation was assessed by MDA test. After treatment for 24 hours by EPX with the
319 indicated concentrations (12, 25 and 50 μ M), a strong elevation in the MDA levels occurs,

320 from 0.502 ± 0.068 $\mu\text{mol MDA/mg}$ of protein for untreated cells to 4.5 ± 0.07 $\mu\text{mol MDA/mg}$
321 of protein for $50 \mu\text{M}$ of EPX (Fig. 4.2).

322

323 The DNA fragmentation in F98 cells after EPX treatment for 24 h was evaluated using the
324 comet test. The score of DNA fragmentation reached about 6.7 folds to the control rate after
325 24 h of EPX intoxication at the strongest dose. Also, as presented in Fig. 4.3, EPX produced
326 100 ± 2.55 , 190 ± 3.7 and 270 ± 2.8 of total rate of DNA damage at doses of 12, 25 and 50
327 μM respectively, as compared to 40 ± 2.07 in untreated cells.

328

329 **3.5. Evaluation of the antioxidant effect of N-acetylcysteine (NAC) on EPX-induced cell**
330 **mortality and apoptotic levels.**

331

332 To determine whether the oxidative stress represents the main cause of the toxicity induced by
333 this pesticide, NAC has been used as an antioxidant against the toxicity of this fungicide.
334 Indeed, F98 cells are pre-treated with NAC (1 mM) during 2 hours before treatment with
335 EPX. As shown in Fig. 5, NAC strongly prevents the cells' viability that has been inhibited by
336 the exposure to increased concentrations of EPX and it also decreases EPX-induced apoptotic
337 levels by analysis of flow cytometry.

338

339

340

341 4. Discussion

342

343 Exposure to chemicals such as pesticides can lead to severe neurologic effects to humans
344 (Costa et al., 2008). Fungicides can damage the brain affecting its functionality (Tabassum et
345 al., 2016). Due to their fat-soluble character, triazole fungicides including EPX can easily
346 cross the blood-brain barrier and the placental barrier (Heusinkveld et al., 2013). They can
347 lead to post-implantation loss and change in body weight offspring during pregnancy (Taxvig
348 et al., 2007). Previous reports showed a close relationship between cell cycle inhibition,
349 apoptosis and cell proliferation in mammals systems (Trivedi et al., 2005; Okamoto et al.,
350 2007 and Liang et al., 2009).

351 Apoptosis is a vital process to normal embryonic development. It is controlled by several
352 effectors and it intervenes in any phase of the cell cycle in order to eliminate surplus or
353 unwanted cells (Raff, 1998; Hengartner, 2000; Kaufmann and Hengartner, 2001). However,
354 there is a lack of data to indicate the link between the decrease of cell proliferation, the
355 inhibition of cell cycle and the programmed cell death in neuronal cells following EPX
356 treatment. In this work, we investigated the possible effects induced by EPX on F98 cells *in*
357 *vitro* on cell proliferation inhibition, cell cycle arrest, cytoskeleton disruption, DNA damage,
358 apoptosis, and ROS generation.

359 In order to evaluate the cytotoxicity of EPX, we firstly assessed the effect of different doses of
360 EPX on the viability of F98 cells. The results showed an inhibition of cell viability in a dose
361 dependent manner with an IC₅₀ of 50 μM of EPX. The arrest of the cell cycle is a control
362 process when cytoskeletal or DNA lesions occur. Cell cycle was detected by flow cytometry
363 and the results of the present work showed that EPX could trigger arrest in G1/S phase at low
364 doses (¼ IC₅₀ and ½ IC₅₀), however with IC₅₀, it produced an accumulation of cells in
365 G2/M phase.

366 A very important relationship between the cell cycle and the organization of cytoskeleton is
367 crucial to ensure the proper functioning of the cell. The immunocytochemical analysis clearly
368 showed that EPX could strongly destroy the cytoskeletal organization with formation of
369 aggregates of microfilaments, intermediate filaments and microtubules. At 50 μM of EPX, the
370 cytoskeleton disappeared, which may be the cause or the result of oxidative damage. These
371 results are similar to previous studies showing the role of oxidative stress in inducing
372 profound structural modifications on the cytoskeleton (Bellomo et al., 1990; Hinshaw et al.,
373 1991; Dent and Gertler, 2003; De Lima Pelaez et al., 2007; Loureiro et al., 2010), and the cell

374 morphology (Gourlay and Ayscough, 2005; Funchal et al., 2006). Indeed, fragmentation of
375 DNA is a powerful inducer of the apoptotic process. The results of this work clearly indicated
376 that EPX intoxication for 24 hours produces important DNA fragmentation in F98 cells, as
377 previously shown in HCT116 cells (Hamdi et al. 2018). Apoptosis can occur by two
378 pathways, including the extrinsic pathway through the death receptor, and the intrinsic
379 pathway through mitochondria (Evan, 1997). The most important features of the intrinsic
380 apoptotic pathway are mitochondrial depolarization and cytochrome-c leakage followed by
381 caspases activation (Garrido et al., 2006).

382 After 24 h of treatment by EPX, we showed a significant inhibition of cell viability which was
383 accompanied by a significant depolarization of mitochondria. Indeed, cell pre-treatment with
384 the caspases inhibitor, ZVAD-fmk, produced a significant inhibition of cell mortality, thus
385 confirming the role of caspases in EPX-induced programmed cell death.

386 Further, for detection of apoptotic cells, a mixture of two dyes (acridine orange and ethidium
387 bromide) was used for morphological cellular changes. When the cell will trigger a
388 programmed death process, several morphological observations will be produced, like
389 condensation of cytoplasm and DNA fragmentation, followed by the degradation of nuclei
390 (Rello et al., 2005; Ndozangue-Tou riguine et al., 2008). Our results showed that the presence
391 of EPX during 24 hours enhances the rate of apoptotic cells. For confirmation of apoptosis,
392 Annexin V-FITC co-staining with propidium iodide was used. The results of our study
393 indicated that EPX induces apoptosis in F98 cells with a concentration-dependent manner.
394 Our data are in agreement with similar studies on bovine lymphocytes (Schwarzbacherova et
395 al. 2017). The authors recorded an increase in the percentage of apoptosis after 24 h treatment
396 by the fungicide Tango® (combination of Epoxiconazole and Fenpropimorph). Moreover,
397 free radicals can easily attack the brain because of its high metabolic rate, high
398 polyunsaturated fatty acids content and low antioxidant rate (Yaduvanshiet al., 2010). We
399 have shown that the treatment of F98 cells by EPX for 24 hours causes a sharp increase in
400 ROS levels inside the cell in a dose-dependent manner. Given its role in many metabolic
401 processes, mitochondrion constitutes an important source of ROS production and is also a
402 vulnerable target of ROS (Liesa et al., 2009, Cho et al., 2010). ROS can attack membrane
403 lipids inducing damage to biological molecules followed by cell death. MDA is considered as
404 a biomarker of lipid peroxidation (Vaca et al., 1988). In our findings, treatment with EPX
405 during 24 hours induced a significant increase in the MDA levels. Toni et al. (2011) reported
406 that Tebuconazole, another triazole pesticide, increases MDA levels after acute exposure (96
407 h) in common carp (*Cyprinus carpio*). Several studies have shown the beneficial effect of N-

408 acetylcysteine (NAC) in various diseases (Arakawa, 2007). NAC plays the role of a precursor
409 of GSH synthesis in cells (Neuwelt et al., 2001). In this study, we assessed the antioxidant
410 effect of NAC on F98 cells. Our results have shown that NAC strongly restores the viability
411 of F98 cells that was inhibited by EPX treatment and it also decreases EPX-induced apoptotic
412 levels by analysis of flow cytometry. This confirms the involvement of ROS in cell cycle
413 arrest, cytoskeletal perturbation, DNA fragmentation, mitochondrial depolarization, apoptosis
414 and lipid oxidation. These results are consistent with previous studies indicating that NAC has
415 a neuroprotective effect against neuronal degeneration (He et al., 2012, Karalija et al., 2012).
416 Similar to other fungicides (fluconazole, itraconazole, voriconazole), which are already used
417 in clinic for human mycoses and as non-steroidal antioestrogens in the treatment of oestrogen-
418 responsive breast tumours in postmenopausal women, EPX is an inhibitor of aromatases and
419 estrogen synthesis. The present study shows that EPX is especially effective on glioblastoma
420 cells. Thus, we are thinking to encapsulate EPX in nanocapsules functionalized with the NFL
421 peptide that targets the entry of nanocapsules into glioblastoma cells (Balzeau et al, 2013,
422 Laine et al 2013). To our knowledge, there is no literature of which we are aware that
423 describes adverse effects associated with agricultural triazole (Epoconazole) exposure in
424 human populations, and in particular the pharmacokinetics of EPX in human brain.
425 Preliminary data show the ability of EPX in affecting *in-vitro* the fundamental characters of
426 neural stem cells isolated from rats by inhibiting the formation and self-renewal of
427 neurospheres, cytoskeleton degradation and inhibition of their cell cycle (data not shown).

428
429 Taken together, we demonstrate for the first time that EPX is heavily toxic against F98 cells,
430 showing a clear effect on cell viability, inducing cell cycle arrest, cytoskeleton
431 disorganization and DNA damage. It also provoked nuclear condensation and fragmentation,
432 decreased the mitochondrial membrane potential and induced apoptosis via caspases
433 dependent signaling pathway. As the apoptotic effect in F98 cells seems to be related to the
434 oxidative stress generation, the use of preventive strategies to minimize the increased
435 production of ROS is the best solution for controlling the toxicity of EPX.

436

437

438 **Conflict of interest**

439

440 The authors declare that there is no conflict of interest.

441

442

443

444

445

446

447

448

449

450 **5. References**

- 451
452 Alverca, E., Andrade, M., Dias, E., Bento, F. S., Batoreu, M. C. C., Jordan, P., Silva, M. J.,
453 Pereira, P., 2009. Morphological and ultrastructural effects of microcystin-LR from
454 *Microcystis aeruginosa* extract on a kidney cell line. *Toxicol.* 54, 283-294.
- 455 Arakawa, M., Ito, Y., 2007. N-acetylcysteine and neurodegenerative diseases. *Basic and*
456 *clinical pharmacology. Cerebellum.* 6, 308-314.
- 457 Balzeau, J., Peterson, A., Eyer, E., 2012. The vimentin-tubulin binding site peptide (Vim-
458 TBS.58-81) crosses the plasma membrane and enters the nuclei of human glioma cells.
459 *International Journal of Pharmaceutics.* 423, 77-83.
- 460 Balzeau, J., Pinier, M., Berges, R., Saulnier, P., Benoit, J.-P., & Eyer, J. (2013). The effect of
461 functionalizing lipid nanocapsules with NFL-TBS.40-63 peptide on their uptake by
462 glioblastoma cells. *Biomaterials,* 34, 3381-3389.
- 463 Barzilai, A., Yamamoto, K. I., 2004. DNA damage responses to oxidative stress. *DNA*
464 *Repair.* 3, 1109-1115.
- 465 Bellomo, G., Mirabelli, F., Vairetti, M., Iosi, F., Malorni, W., 1990. Cytoskeleton as a target
466 in menadione-induced oxidative stress in cultured mammalian cells. I. Biochemical and
467 immunocytochemical features. *Journal of Cellular Physiology.* 143, 118-128.
- 468 Cao, J., Liu, Y., Jia, L., Zhou, H.M., Kong, Y., Yang, G., Jiang, L.P., Li, Q.J., Zhong, L.F.,
469 2007. Curcumin induces apoptosis through mitochondrial hyperpolarization and mtDNA
470 damage in human hepatoma G2 cells. *Free Radical Biology and Medicine.* 43, 968-975.
- 471 Cathcart, R. Schwiers, E., Ames, B.N., 1983. Detection of picomole levels of hydroperoxides
472 using a fluorescent dichlorofluorescein assay. *Analytical Biochemistry.* 134, 111-116.
- 473 Cho, D.H., Nakamura, T., Lipton, S.A., 2010. Mitochondrial dynamics in cell death and
474 neurodegeneration. *Cellular and Molecular Life Sciences.* 67, 3435-3447.
- 475 Costa, L.G., Giordano, G., Guizzetti, M., Vitalone, A., 2008. Neurotoxicity of pesticides: a
476 brief review. *Frontiers in Bioscience.* 13, 1240-1249.
- 477 De Lima Pelaez, P., Funchal, C., Loureiro, S. O., Heimfarth, L., Zamoner, A., Gottfried, C.,
478 Latini, A., Wajner, M., Pessoa-Pureur, R., 2007. Branched-chain amino acids
479 accumulating in maple syrup urine disease induce morphological alterations in C6
480 glioma cells probably through reactive species. *International Journal of Developmental*
481 *Neuroscience.* 25, 181-189.
- 482 De Wilde, T., Spanoghe, P., Debaer, C., Ryckeboer, J., Springael, D., Jaeken, P., 2007.
483 Overview of on-farm bioremediation systems to reduce the occurrence of point source
484 contamination. *Pest Management Science.* 63, 111-128.
- 485 Debbasch, C., Brignole, F., Pisella, P.J., Warnet, J.M., Rat, P., Baudouin, C., 2001.
486 Quaternary ammoniums and other preservatives' contribution in oxidative stress and
487 apoptosis on Chang conjunctival cells. *Investigative, Ophthalmology and Visual*
488 *Science,* 42, 642-652.
- 489 Dent, E. W., Gertler, F. B., 2003. Cytoskeletal dynamics and transport in growth cone motility
490 and axon guidance. *Neuron.* 40, 209-227.
- 491 Ding, W.X., Shen, H.M., Ong, C.N., 2006b. Microcystic cyanobacteria extract induces
492 cytoskeletal disruption and intracellular glutathione alteration in hepatocytes.
493 *Environmental Health Perspectives.* 108, 605-609.
- 494 El-Amrani, S., Pena-Abaurrea, M., Sanz-Landaluze, J., Ramos, L., Guinea, J., Amara, C.,
495 2012. Bioconcentration of pesticides in zebrafish eleutheroembryos (*Danio rerio*).
496 *Science of the Total Environment.* 425, 184-190.
- 497 EPA (2006). Reregistration eligibility decision for triadimefon and tolerance reassessment for
498 triadimenol, Washington.

- 499 Evan, G., 1997. Cancer a matter of life and cell death. *International Journal of Cancer*.71,
500 709-711.
- 501 Funchal, C., Latini, A., Jacques-Silva, M. C., Dos Santos, A. Q., Buzin, L., Gottfried, C.,
502 Wajner, M., Pessoa-Pureur, R., 2006. Morphological alterations and induction of
503 oxidative stress in glial cells caused by the branched-chain alpha-keto acids
504 accumulating in maple syrup urine disease. *Neurochemistry International*. 49, 640-650.
- 505 Garrido, C., 2006. Mechanisms of cytochrome c release from mitochondria. *Cell Death and*
506 *Differentiation*. 13, 1423-1433.
- 507 Ghannoum, M., Rice, L., 1999. Antifungal Agents: Mode of action, mechanisms of resistance,
508 and correlation of these mechanisms with bacterial resistance. *Clinical Microbiology*
509 *Reviews*. 12, 501-517.
- 510 Gomes, A., Fernandes, E., Lima, J. L., 2005. Fluorescence probes used for detection of
511 reactive oxygen species. *Biochemical and Biophysical Methods*. 65, 45-80.
- 512 Gourlay, C. W., Ayscough, K. R., 2005a. The actin cytoskeleton in ageing and apoptosis.
513 *FEMS Yeast Research*. 5, 1193-1198.
- 514 Gourlay, C. W., Ayscough, K. R., 2005b. The actin cytoskeleton: a key regulator of apoptosis
515 and ageing? *Nature Reviews Molecular Cell Biology*. 6, 583-589.
- 516 Hamdi, H., Ben Salem, I., Ben Othmène, Y., Annabi, E., Abid-Essefi, S., 2018. The
517 involvement of ROS generation on Epoxiconazole-induced toxicity in HCT116 cells.
518 *Pesticide Biochemistry and Physiology*. 148, 62-67.
- 519 He, S.J. Hou, J.F., Dai, Y.Y., Zhou, Z.L., Deng, Y.F., 2012. N-acetyl-cysteine protects
520 chicken growth plate chondrocytes from T-2 toxin induced oxidative stress. *Applied*
521 *Toxicology*. 32, 980–985.
- 522 Hengartner, M.O., 2000. The biochemistry of apoptosis. *Nature*. 407, 770-776.
- 523 Hester, S., Moore, T., Padgett, W.T., Murphy, L., Wood, Ch.E., Nesnow, S., 2012. The
524 Hepatocarcinogenic Conazoles: Cyproconazole, Epoxiconazole, and Propiconazole
525 Induce a Common Set of Toxicological and Transcriptional Responses. *Toxicological*
526 *Sciences*. 127, 54–65.
- 527 Hester, S.D. Wolf, D.C., Nesnow, S.S., Thai, F., 2006. Transcriptional profiles in liver from
528 rats treated with tumorigenic and non-tumorigenic triazole conazole fungicides:
529 propiconazole, triadimefon, and myclobutanil. *Toxicologic Pathology*. 34, 879–894.
- 530 Heusinkveld, H. J., Molendijk, J., van den Berg, M., Westerink, R. H. S., 2013. Azole
531 Fungicides Disturb Intracellular Ca²⁺ in an Additive Manner in Dopaminergic PC12
532 Cells. *Toxicological sciences*. 134, 374–381.
- 533 Hinshaw, D. B., Burger, J. M., Beals, T. F., Armstrong, B. C., Hyslop, P. A., 1991. Actin
534 polymerization in cellular oxidant injury. *Archives of Biochemistry and Biophysics*.
535 288, 311–316.
- 536 Hooser, S.B., Beasley, V.R., Waite, L.L., Kuhlenschmidt, M.S., Carmichael, W.W., Haschek,
537 W.M., 1991. Actin filament alterations in rat hepatocytes induced in vivo and in vitro by
538 microcystin-LR, a hepatotoxin from the blue-green alga, *Microcystis aeruginosa*.
539 *Veterinary Pathology*. 28, 259–266.
- 540 Hu, K., Yang, M., Xu, Y.Y., Wei, K., Ren, J., 2015. Cell Cycle Arrest, Apoptosis, and
541 Autophagy Induced by Chabamide in Human Leukemia Cells. *Chinese Herbal*
542 *Medicines*. 8, 30-38.
- 543 Karalija, A., Novikova, L. N., Kingham, P. J., Wiberg, M., Novikov, L. N., 2012.
544 Neuroprotective effects of N-acetylcysteine and Acetyl-L-Carnitine after spinal cord
545 injury in adult rats. *PLoS ONE*. 7, e41086.
- 546 Karanasios, E., Tsiropoulos, N.G., Karpouzias, D.G., 2012. On-farm biopurification systems
547 for the depuration of pesticide wastewaters: recent biotechnological advances and future
548 perspectives. *Biodegradation*. 23, 787-802.

- 549 Kaufmann, S.H., Hengartner, M.O., 2001. Programmed cell death alive and well in the new
550 millennium. *Trends in Cell Biology*. 11, 526-534.
- 551 Lainé, A.-L., Adriaenssens, E., Vessières, A., Jaouen, G., Corbet, C., Desruelles, E., ...
552 Passirani, C. (2013). The in vivo performance of ferrocenyl tamoxifen lipid
553 nanocapsules in xenografted triple negative breast cancer. *Biomaterials*, 34(28), 6949–
554 6956.
- 555 Le Bel, C.P., Ischiropoulos, H., Bondy, S.C., 1992. Evaluation of the probe 2-,7-
556 dichlorofluorescein as an indicator of reactive oxygen species formation and oxidative
557 stress, *Chemical Research in Toxicology*. 5, 227–31.
- 558 Li, S., 2013. Avermectin exposure induces apoptosis in King pigeon brain neurons.
559 *Pesticide Biochemistry and Physiology*. 107, 177–187.
- 560 Li, X.Y., Liu, Y.D., Song, L.R., 2001. Cytological alterations in isolated hepatocytes from
561 common carp (*Cyprinus carpio* L.) exposed to microcystin-LR.
562 *Environmental Toxicology*. 16, 517–522.
- 563 Liang, Q., Xiong, H., Zhao, Z., Jia, D., Li, W., Qin, H., Deng, J., Gao, L., Zhang, H., Gao, G.,
564 2009. Inhibition of transcription factor STAT5b suppresses proliferation, induces G1 cell
565 cycle arrest and reduces tumor cell invasion in human glioblastoma multiforme cells.
566 *Cancer Letters*. 273, 164-171.
- 567 Liesa, M., Palacin, M., Zorzano, A., 2009. Mitochondrial dynamics in mammalian health and
568 disease. *Physiological Reviews*, 89, 799-845.
- 569 Livingstone, D., 2001. Contaminant-stimulated reactive oxygen species production and
570 oxidative damage in aquatic organisms. *Marine Pollution Bulletin*. 42, 656-666.
- 571 Loureiro, S.O., Heimfarth, L., Pelaez Pde, L., Lacerda, B.A., Vidal, L.F., Soska, A.,
572 Santos, N.G., Andrade, C., Tagliari, B., Scherer, E.B., Guma, F.T., Wyse, A.T.,
573 Pessoa-Pureur, R., 2010. Hyperhomocysteinemia selectively alters expression and
574 stoichiometry of intermediate filament and induces glutamate- and calciummediated
575 mechanisms in rat brain during development. *International Journal of*
576 *Developmental Neuroscience*. 28, 21–30.
- 577 Mirza, M. B., Elkady, A. I., Al-Attar, A. M., Syed, F. Q., Mohammed, F. A., Hakeem, K. R.,
578 2018. Induction of apoptosis and cell cycle arrest by ethyl acetate fraction of *Phoenix*
579 *dactylifera* L. (Ajwadates) in prostate cancer cells. *Journal of Ethnopharmacology*. 218,
580 35-44.
- 581 Mukhtar, E., Adhami, V.M., Mukhtar, H., 2014. Targeting microtubules by natural agents for
582 cancer therapy. *Molecular Cancer Therapeutics*. 13, 275–284.
- 583 Ndozangue-Touriguine, O., Hamelin, J., Breard, J., 2008. Cytoskeleton and apoptosis.
584 *Biochemical Pharmacology*. 76, 11–18.
- 585 Neuwelt, E. A., Pagel, M. A., Hasler, B. P., Deloughery, T. G., Muldoon, L. L., 2001.
586 Therapeutic efficacy of aortic administration of N-acetylcysteine as a chemoprotectant
587 against bone marrow toxicity after intracarotid administration of alkylators, with or
588 without glutathione depletion in a rat model. *Cancer research*. 61, 7868-74.
- 589 Ohkawa, H., Ohishi, N., Yagi, K., 1979. Assay for lipid peroxide in animal tissues by
590 thiobarbituric acid reaction. *Analytical Biochemistry*. 95, 351–358.
- 591 Okamoto, S., Kang, Y., Brechtel, C., Siviglia, E., Russo, R., Clemente, A., Harrop, A.,
592 McKercher, S., Kaul, M., Lipton, S., 2007. HIV/gp120 decreases adult neural progenitor
593 cell proliferation via checkpoint kinase-mediated cell-cycle withdrawal and G1 arrest.
594 *Cell Stem Cell*. 1, 230-236.
- 595 Raff, M., 1998. Cell suicide for beginners. *Nature*. 396, 119-12.
- 596 Rello, S., Stockert, J.C., Moreno, V., Gámez, A., Pacheco, M., Juarranz, A., Canete, M.,
597 Villanueva, A., 2005. Morphological criteria to distinguish cell death induced by
598 apoptotic and necrotic treatments. *Apoptosis*. 10, 201-208.

599 Ross, J. A., Moore, T., Leavitt, S. A., 2009. In vivo mutagenicity of conazole fungicides
600 correlates with tumorigenicity. *Mutagenesis*. 24, 149-152.

601 Ross, J. A., Leavitt, S. A., Schmid, J. E., Nelson, G. B., 2012. Quantitative changes in
602 endogenous DNA adducts correlate with conazole in vivo mutagenicity and
603 tumorigenicity. *Mutagenesis*. 27, 541-549.

604 Santosh, K., Yaduvanshi, K., Ojha, A., Pant, S. C., Lomash, V., Srivastava, N., 2010.
605 Monocrotophos induced lipid peroxidation and oxidative DNA damage in rat tissues.
606 *Pesticide Biochemistry and Physiology*. 97, 214-222.

607 Schwarzbacherová, V., Wnuk, M., Lewinska, A., Potocki, L., Zebrowski, J.,
608 Kozirowskie, M., Holečková, B., Šiviková, K., Dianovská, J., 2017. Evaluation of
609 cytotoxic and genotoxic activity of fungicide formulation Tango® Super in bovine
610 lymphocytes. *Environmental Pollution, Part A*. 220, 255-263.

611 Šiviková, K., Holečková, B., Schwarzbacherová, V., Galdíková, M., Dianovský, J., 2018.
612 Potential chromosome damage, cell-cycle kinetics/and apoptosis induced by
613 epoxiconazole in bovine peripheral lymphocytes in vitro. *Chemosphere*. 193, 82-88.

614 Tabassum, H., Khan, J., Salman, M., Raisuddin, S., Parvez, S., 2016. Propiconazole induced
615 toxicological alterations in brain of freshwater fish *Channa punctata* Bloch. *Ecological*
616 *Indicators*. 62. 242-248.

617 Taxvig, C., Hass, U., Axelstad, M., 2007. Endocrine-disrupting activities in vivo of the
618 fungicides tebuconazole and epoxiconazole. *Toxicological Sciences*, 100, 464-73.

619 Toni, C., Ferreira, D., Kreutz, L.C., Loro, V. L., Barcellos, L.J., 2011a. Assessment of
620 oxidative stress and metabolic changes in common carp (*Cyprinus carpio*) acutely
621 exposed to different concentrations of the fungicide tebuconazole. *Chemosphere*. 83,
622 579-584.

623 Toni, C., Loro, V.L., Santi, A., de Menezes, C.C., Cattaneo, R., Clasen, B.E., Zanella, R.,
624 2011b. Exposure to tebuconazol in rice field and laboratory conditions induces oxidative
625 stress in carp (*Cyprinus carpio*). *Comparative Biochemistry and Physiology - Part C:*
626 *Toxicology & Pharmacology*. 153, 128-132.

627 Trivedi, P.P., Roberts, P.C., Wolf, N.A., Swanborg, R.H., 2005. NK cells inhibit T cell
628 proliferation via p21-mediated cell cycle arrest. *Journal of Immunology*. 174, 4590-
629 4597.

630 Trosken, E. R., Scholz, K., Lutz, R.W., Volkel, W., Zarn, J.A., Lutz, W. K., 2004.
631 Comparative assessment of the inhibition of recombinant human CYP19 (aromatase) by
632 azoles used in agriculture and as drugs for humans. *Endocrine Research*. 30, 387-94.

633 Tully, D. B., Bao, W., Goetz, A. K., Blystone, C. R., Ren, H., Schmid, J. E., Strader, L. F.,
634 Wood, C. R., Best, D. S., Narotsky, M. G., Wolf, D., Rockett, C. J. C., Dix, D. J., 2006.
635 Gene expression profiling in liver and testis of rats to characterize the toxicity of triazole
636 fungicides. *Toxicology and Applied Pharmacology*. 215, 260-273.

637 Vaca, C. E., Wilhelm, J., Harms-Ringdahl, M., 1988. Interaction of lipid peroxidation product
638 with DNA. *Mutation Research*, 195, 137-149.

639 Verweij, P.E., Kema, G.H.J., Zwaanc, B., Melchersa, W.J.G., 2013. Triazole fungicides and
640 the selection of resistance to medical triazoles in the opportunistic mould *Aspergillus*
641 *fumigates*. *Pest Management Science*. 69, 165-170.

642 Wang, W., Xiong, W., Wan, J.L., Sun, X.H., Xu, H.B., Yang, X.L., 2009. The decrease of
643 PAMAM dendrimer-induced cytotoxicity by PEGylation via attenuation of oxidative
644 stress. *Nanotechnology*. 20, 103-105.

645 Wuttke, W., Pitzel, L., Seidlova-Wuttke, D., Hinney, B., 2001. LH pulses and the corpus
646 luteum: the luteal phase deficiency (LPD). *Vitamins Hormones*. 63, 131-158.

647

648 **6. Figure legends**

649

650 **Fig. 1.** Cytotoxic effects and apoptosis induced by EPX on F98 cells. The effect of treating
651 F98 cells with these increasing concentrations of EPX (12 μ M, 25 μ M and 50 μ M) for 24 h
652 was evaluated using MTT test. Each experiment was repeated 3 times under different
653 treatment conditions and data are expressed as the mean \pm SD. Values are significantly
654 different ($p < 0.05$) from control (**Fig. 1.1**).

655

656 The quantification of F98 cells in the different cell cycle phases after treatment with EPX at
657 the different concentrations was done using flow cytometric analysis (**Fig. 1.2.B**). Each
658 experiment was repeated 3 times and data are expressed as the mean \pm SD. Values are
659 significantly different from control (* $p < 0.05$; ** $p < 0.001$).

660

661 The effect of EPX in cell apoptosis of F98 cells. Morphological changes such as chromatin
662 condensation and nucleus degradation are key features of apoptosis. Images are taken by
663 fluorescence microscopy using AO/EB dyes combination (**Fig. 1.3.A**). The control cells are
664 stained green, the dead cells by early apoptosis are stained light green, the dead cells by late
665 apoptosis are stained orange and the necrotic cells are stained red. Each experiment was
666 repeated 3 times under different treatment conditions and data are expressed as the mean \pm
667 SD. * $P < 0.05$ and ** $P < 0.01$ vs. the negative control (**Fig. 1.3.B**). The apoptosis of cells was
668 also confirmed by Annexin-V/PI double-staining after EPX treatment for 24 hours. The rate
669 of apoptosis cells was assessed as means \pm SD. of three experiments done separately. * $P < 0.05$
670 and ** $P < 0.01$ vs the negative control (**Fig. 1.4.A, B**).

671

672 **Fig. 2.** Effect of IC50 of EPX on the cytoskeleton of F98 cells. Microscopic examination
673 using confocal microscopy shows aggregation of microtubules (MTs), intermediate filaments
674 (IFs) and actin microfilaments (MFs) following EPX treatment. Cells treated with 50 μ M
675 EPX have lost their normal cytoskeleton.

676

677 **Fig. 3.** EPX induces depolarization of mitochondria and caspases activation. Treatment of F98
678 cells with EPX for 24 h reduced the mitochondrial potential. Each experiment was repeated 3
679 times under different treatment conditions and data are expressed as the mean \pm SD. Values
680 are significantly different (* $p < 0.05$) (** $p < 0.0001$) from control (**Fig. 3.1**).

681

682 The effect of pre-treatment with caspases inhibitor ZVAD-fmk (2 h, 50 μ M) on the viability
683 of F98 cells after incubation with EPX for 24 hours was evaluated using MTT test. Each
684 experiment was repeated 3 times and data are expressed as the mean \pm SD. Values are
685 significantly different (* p < 0.05); (** p < 0.001) from control. (αp <0.05) values are
686 significantly different from ZVAD-fmk pretreated cells (**Fig. 3.2**).

687

688 **Fig. 4.** Levels of ROS generation, malondialdehyde (MDA) production and score of DNA
689 damage following 24 hours of EPX treatment. The oxidation of DCFH to DCF reflects the
690 amount of ROS produced. Each experiment was repeated 3 times and data are expressed as
691 the mean \pm SD. Values are significantly different (* p < 0.05); (** p < 0.001); (***) p <0.0001
692 from control (**Fig. 4.1**).

693

694 EPX at the indicated concentrations induced lipid oxidation in F98 cells after incubation for
695 24 h. The level of lipid peroxidation is proportional to the rate of malondialdehyde (MDA).
696 Each experiment was repeated 3 times under different treatment conditions and data are
697 expressed as the mean \pm SD. Values are significantly different (* p < 0.05); (** p <0.001);
698 (***) p <0.0001) from control (**Fig. 4.2**).

699

700 Score of DNA fragmentation in F98 cells after incubation for 24 h with EPX at 12 μ M, 25
701 μ M and 50 μ M. Each experiment was repeated 3 times and data are expressed as the mean \pm
702 SD. Values are significantly different (* p < 0.05); (** p < 0.001); (***) p <0.0001) from control
703 (**Fig. 4.3**).

704

705 **Fig. 5.** The effect of NAC (N-acetyl-cysteine) on EPX-induced cell mortality and apoptotic
706 levels. The cell viability was evaluated after pretreatment with NAC (1 mM) using MTT test
707 (**Fig. 5.1**). The rate of EPX-induced apoptotic levels was assessed by analysis of flow
708 cytometry after pretreatment with NAC (1 mM) (**Fig. 5.2.A, B**). Each experiment was
709 repeated 3 times and data are expressed as the mean \pm SD. Values are significantly different
710 (* p <0.05); (** p <0.001) from control, (αp <0.05); ($\alpha\alpha p$ <0.001), values are significantly
711 different from NAC-pretreated cells.

712

713

714

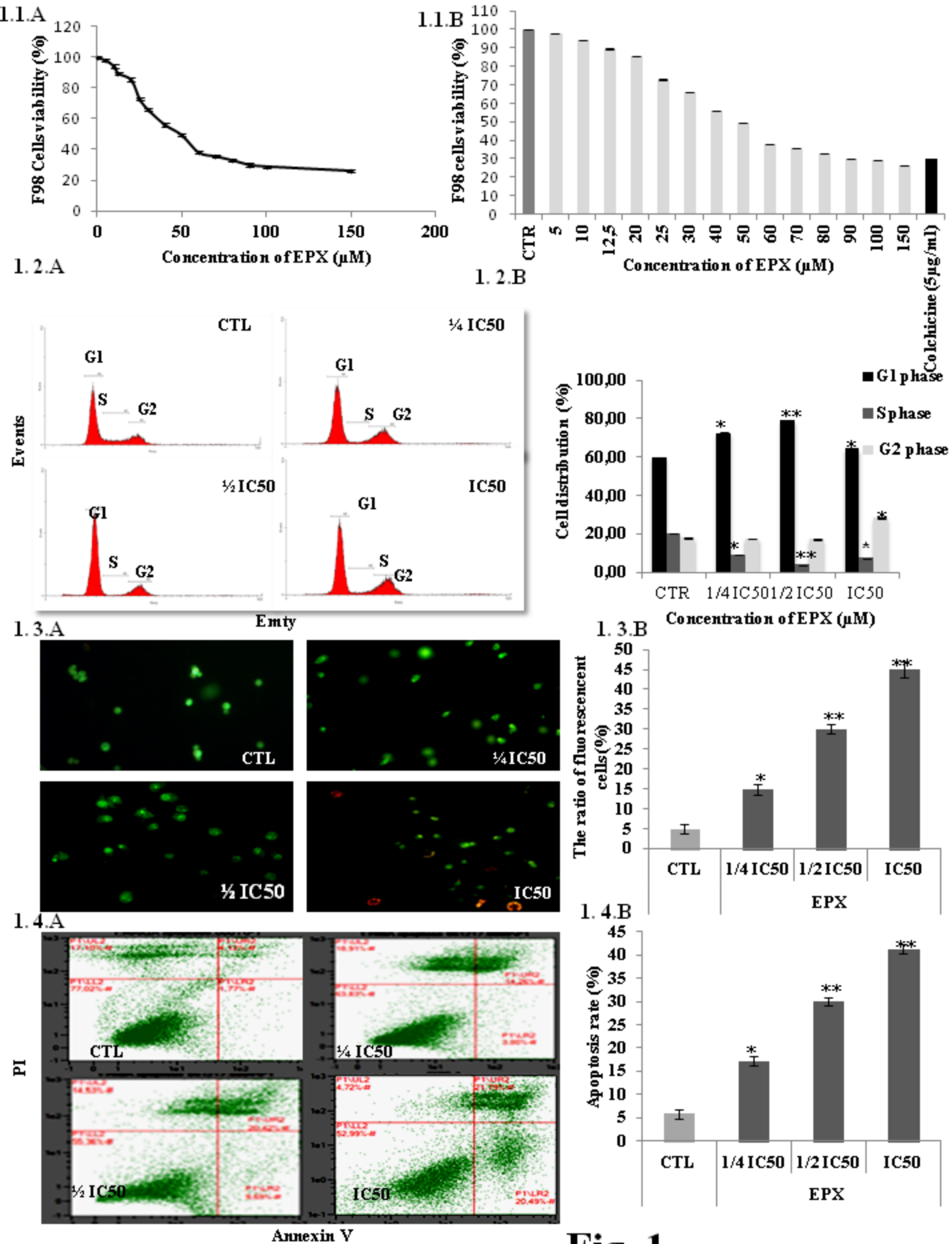


Fig. 1

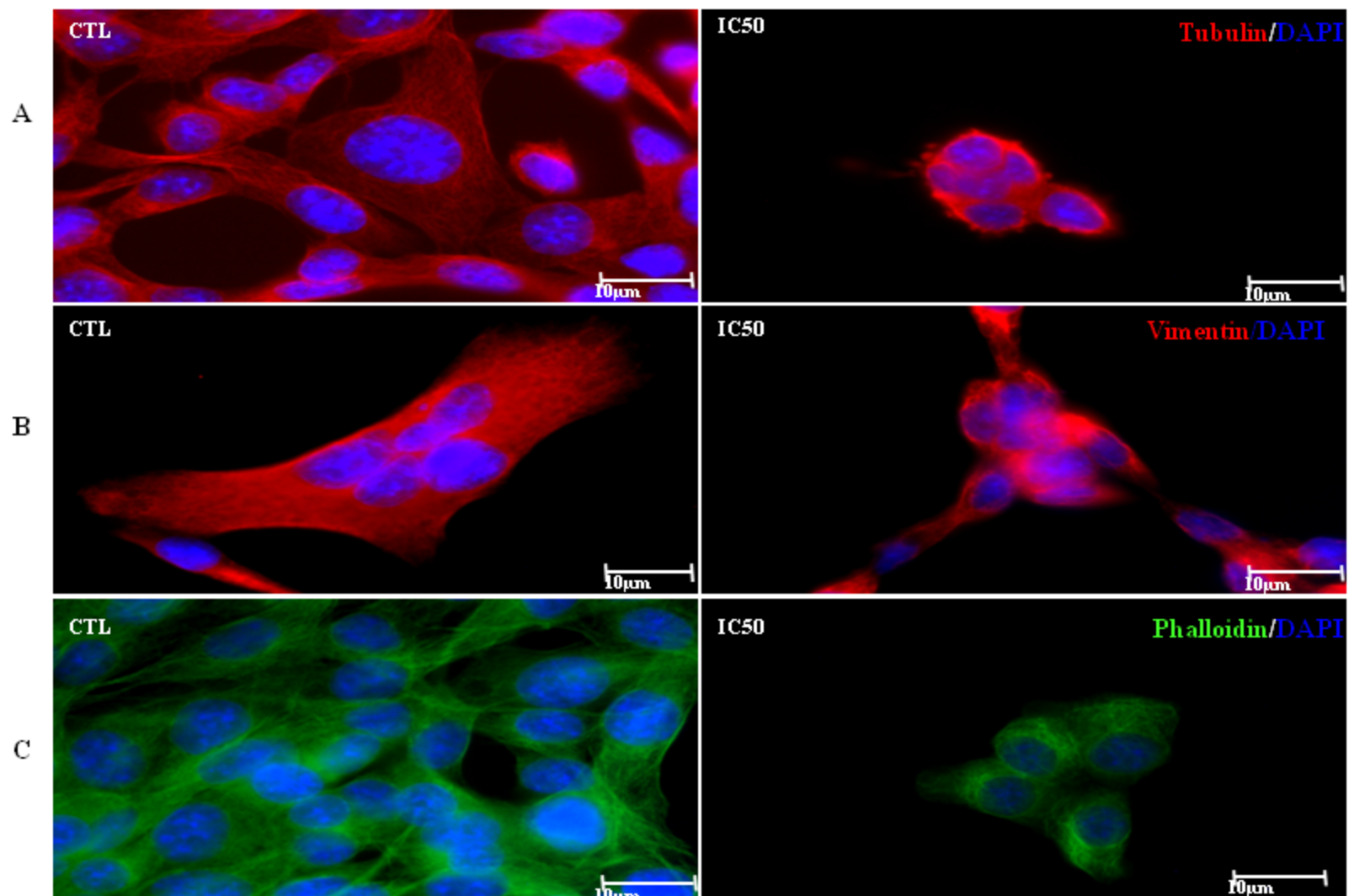
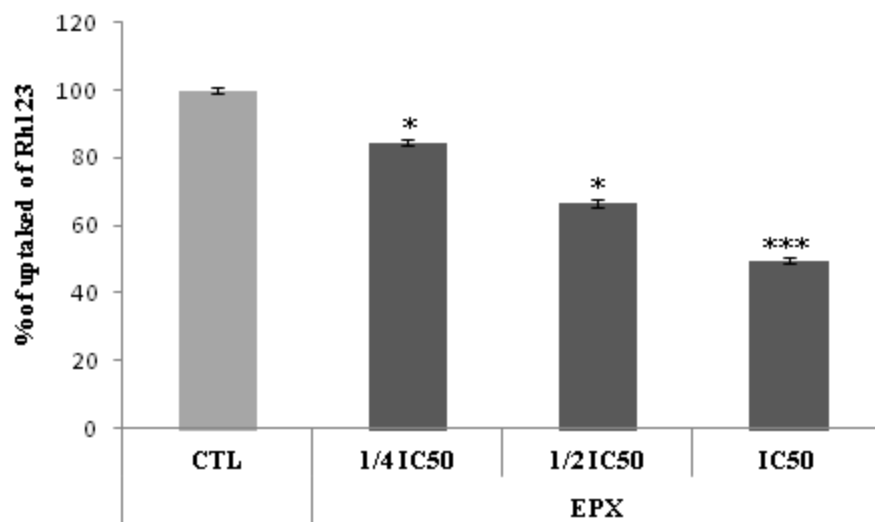


Fig. 2

3.1



3.2

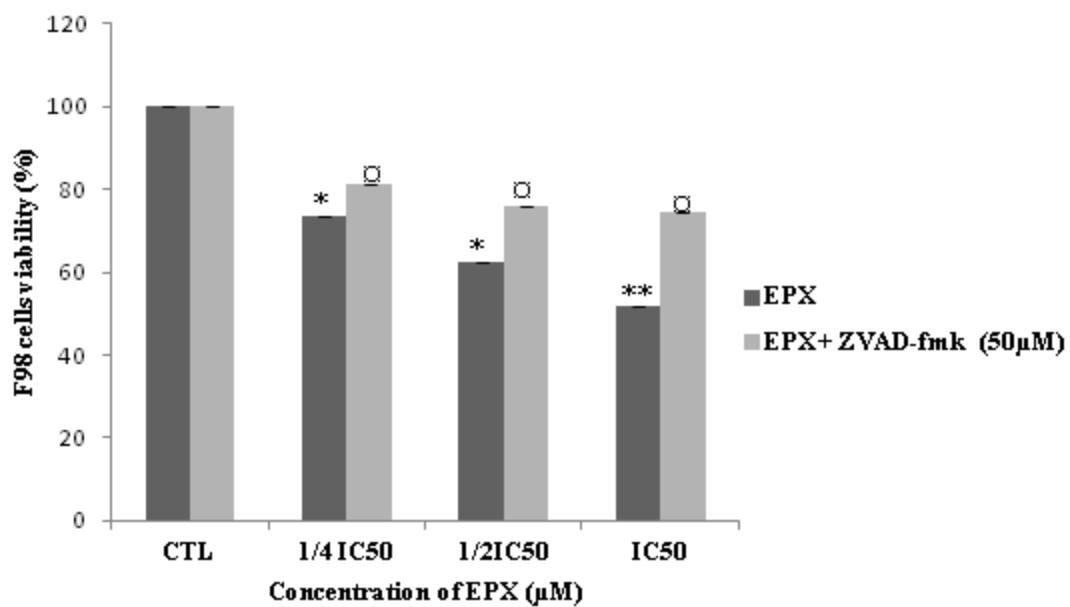
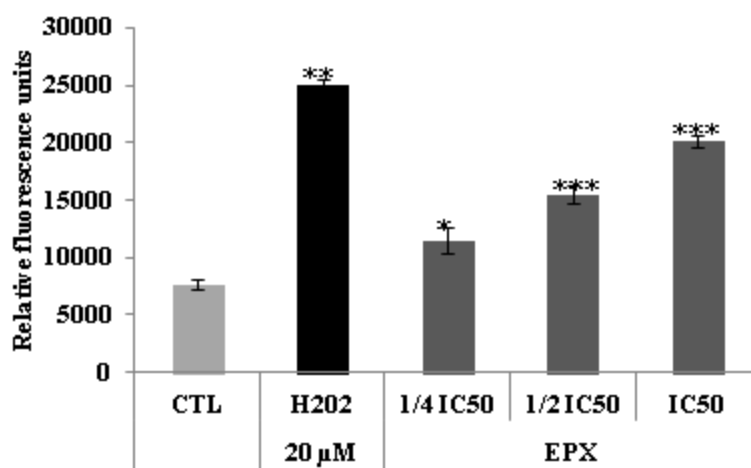
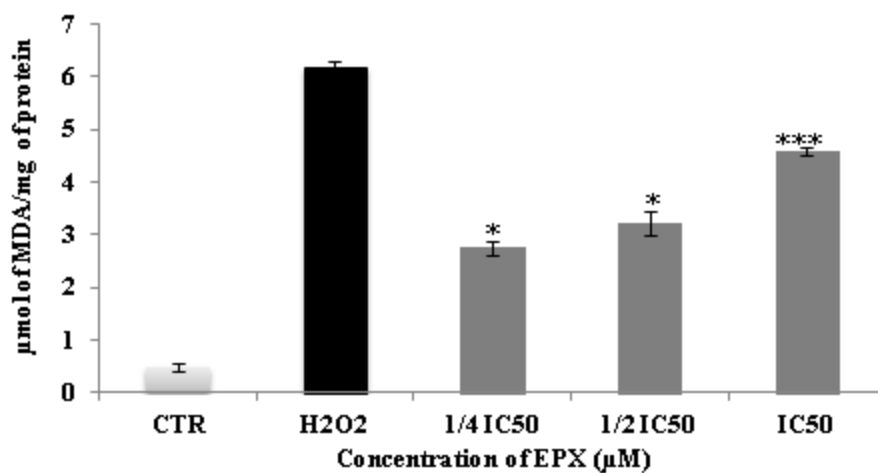


Fig. 3

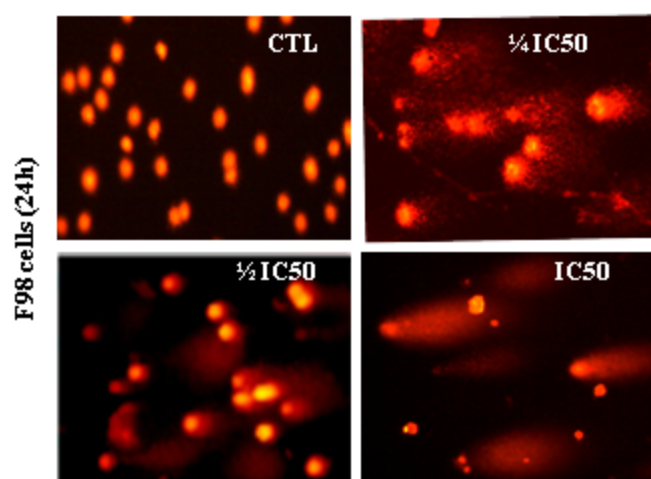
4.1



4.2



4.3.A



4.3.B

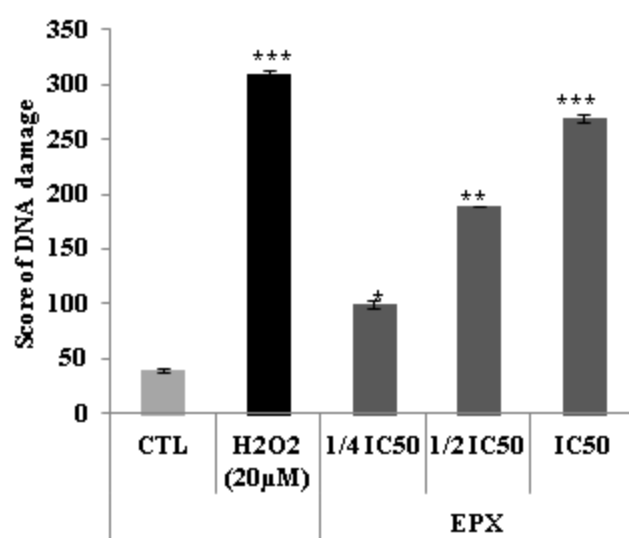
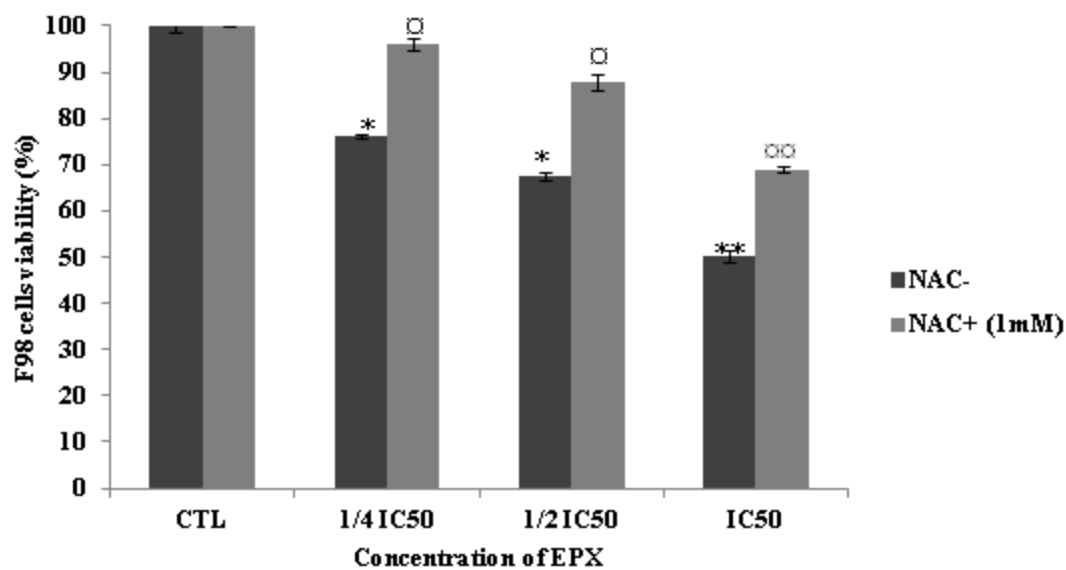


Fig. 4

5.1



5.2.A

5.2.B

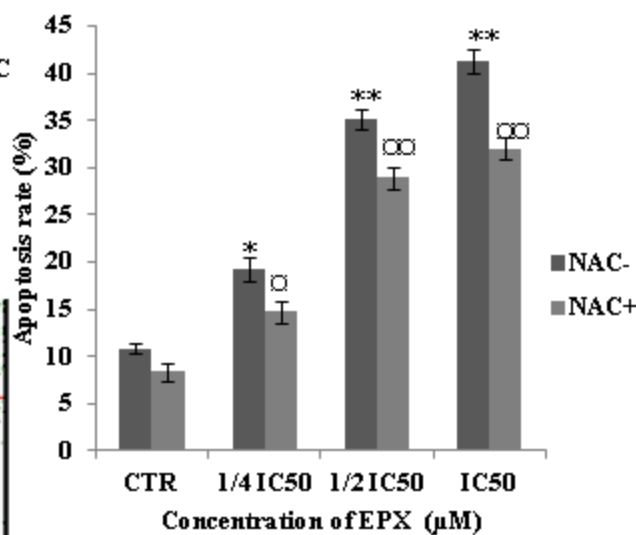
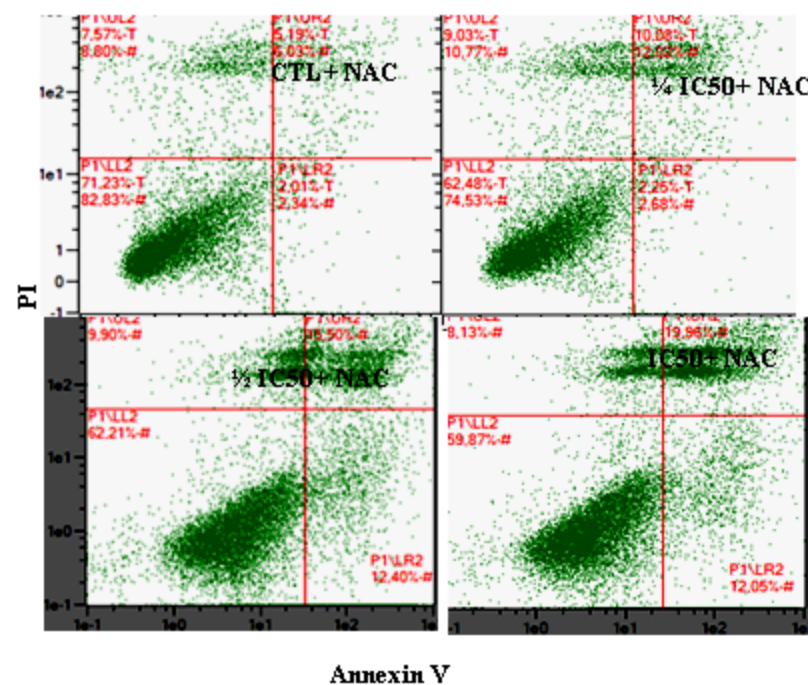
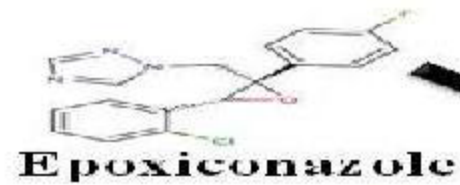


Fig. 5



F98 Cells

**Thiol
NAC**

**ROS
ROS
ROS**

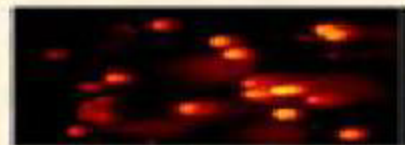
Cytotoxic effect

Formazan

MTT

**Cell
Cycle**

Genotoxic effect



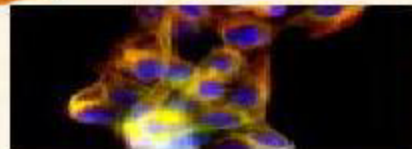
Comet assay

Loss of MMP



Cytoskeleton disruption

**Cell
Proliferation**



Apoptosis

**Caspases
dependent**

